Atmospheric Research 153 (2015) 200–208

Contents lists available at ScienceDirect

Atmospheric Research

journal homepage: www.elsevier.com/locate/atmos

The characteristics of atmospheric ice nuclei measured at the top of Huangshan (the Yellow Mountains) in Southeast China using a newly built static vacuum water vapor diffusion chamber

Hui Jiang [a,b], Yan Yin [a,b,*], Hang Su [b], Yunpeng Shan [b], Renjie Gao [b]

[a] Collaborative Innovation Center on Forecast and Evaluation of Meteorological Disasters, Nanjing University of Information Science & Technology, Nanjing 210044, China
[b] Key Laboratory for Aerosol–Cloud–Precipitation of the China Meteorological Administration, School of Atmospheric Physics, Nanjing University of Information Science and Technology, Nanjing 210044, China

ARTICLE INFO

Article history:
Received 14 May 2014
Received in revised form 29 August 2014
Accepted 29 August 2014
Available online 6 September 2014

Keywords:
Ice nuclei
Static vapor diffusion chamber
Supersaturation
Relative humidity

ABSTRACT

A newly built static vacuum water vapor diffusion chamber was built to measure the concentration of ice nuclei (INs) at the top of Huangshan (the Yellow Mountains) in Southeast China. The experiments were conducted under temperatures between −15 °C and −23 °C and supersaturations with respect to ice between 4% and 25%. The results show that the average IN concentration was in the range of 0.27 to 7.02 L^{-1}, when the temperature was varied from −15 °C to −23 °C. The changes in IN concentrations with time were correlated with the change of number concentration of the aerosol particles of 0.5–20 μm in diameter. The square correlation coefficients (R^2) between IN and coarse aerosol particles (0.5–20 μm in diameter) were all higher than 0.60, much higher than that (0.10) between IN and smaller particles (0.01–0.5 μm). The concentration of ice nuclei at 14:00 LST was significantly higher than that at 08:00 LST, which is correlated with the diurnal variation of the concentration of aerosol particles. A parametric equation was developed based on measurements to represent the variations of IN concentration with temperature and supersaturation.

1. Introduction

Aerosol particles which can generate ice crystals by freezing supercooled water droplets or water vapor deposited on their surface are called ice nuclei (IN). Pure water droplets can remain unfrozen even at temperature of −40 °C, if IN are absent. The presence of atmospheric ice nuclei can greatly increase the ice nucleating temperature. Four types of ice nucleation mechanisms are proposed in natural clouds: deposition nucleation, condensation freezing, immersion freezing, and contact freezing. IN can directly affect the size and number concentration of ice particles in clouds (Hallett and Mason, 1958; Lohmann et al., 2004), thus indirectly affect the formation of precipitation and the lifetime of clouds (Lohmann et al., 2007). The impact of IN on cold cloud properties and formation of precipitation is complex (Gierens, 2003; Haag and Kärcher, 2004; Kärcher, 2004). Haag and Kärcher (2004) proposed that an increase in IN at the upper troposphere can increase the formation rate of cirrus clouds. However, the role of IN in the development of precipitation is still poorly understood, and therefore needs further investigation (Levin and Cotton, 2009).

* Corresponding author at: Key Laboratory for Aerosol–Cloud–Precipitation of China Meteorological Administration, Nanjing University of Information Science & Technology, 219 Ningliu Road, Nanjing 210044, China. Tel.: +86 25 58731207.
E-mail address: yinyan@nuist.edu.cn (Y. Yin).

http://dx.doi.org/10.1016/j.atmosres.2014.08.015

Mineral dust has long been known to be effective in catalyzing ice formation (Roberts and Hallett, 1968; Knopf and Koop, 2006; Field et al., 2006; Niedermeier et al., 2010; Murray et al., 2010). Many laboratory studies demonstrated that mineral dust can nucleate ice at a temperature higher than −38 °C (Pruppacher and Klett, 1997). Some recent work showed that droplets formed on mineral particles covered with sulfate can freeze at temperature as high as −10 °C, which is much higher than the temperature required for freezing pure sulfate droplets (Archuleta et al., 2005; Zuberi et al., 2002). Some studies also found that soot particles (Cozic et al., 2008; Pratt et al., 2009, 2010), biological debris (Pratt et al., 2009; Prenni et al., 2009), volcanic ash particles (Durant et al., 2008; Hoyle et al., 2011; Steinke et al., 2011) and sea salt (Wise et al., 2012) can be used as atmospheric IN. Some previous studies also showed that organic particles (e.g., Froyd et al., 2010; Murray et al., 2010), and marine algae (e.g., Knopf et al., 2011) are also important IN sources. Wang et al. (2012) suggested that atmospheric secondary organic aerosol (SOA) is potentially important for ice cloud formation and climate. The qualitative influence of these compositions on ice nucleation properties was shown in a recent review compiled by Hoose and Möler (2012). Cziczo et al. (2013) determined in situ the composition of the residual particles within cirrus crystals after the ice was sublimated. Their results demonstrated that mineral dust and metallic particles are the dominant source of residual particles, whereas sulfate and organic particles are underrepresented and elemental carbon and biological materials are essentially absent.

A wide variety of techniques have been developed for detecting IN and measuring IN characteristics. For the early Bigg mixing cold cloud chamber (Bigg, 1957), outside air is brought directly into the chamber and the number of IN is measured by counting the number of ice crystals falling into a sugar solution. Some observations were conducted by collecting aerosols on filters and analyzing their ice nucleating properties by exposing them to water saturation conditions at different temperatures in the laboratory, called filter method (Bigg, 1973). Some researchers measured IN concentration by counting the number of supercooled water droplets frozen in a freely-falling freezing tube (e.g., Saxena and Weintraub, 1988; Junge and Swanson, 2008). Continuous flow diffusion chamber (CFDC) has also been widely used for IN measurements (Hussain and Saunders, 1984; Rogers, 1988; DeMott et al., 2003).

Large spatial and temporal variations in IN concentration were observed during different campaigns worldwide. A review of the results of IN measurements in Antarctica was presented in Belosi et al. (2014) where they showed that IN concentrations have significant variations over various locations. Ardon-Dryer et al. (2011) reported immersion freezing nucleus concentrations measured at the South Pole station and found that freezing occurred between −18 °C and −27 °C, with active nucleus concentration of 1 L^{-1} at −23 °C. Saxena and Weintraub (1988) measured IN based on drop freezing at Palmer station and reported that the concentration of IN is 0.03–10 L^{-1} at temperature of −5 °C to −7 °C. They also found a good correlation between the IN concentration and the concentrations of zinc, silicon, and potassium components.

Results from measurements of IN around the world have been published in the past few decades, however, only very few were reported from China (Jiang et al., 2014). Jiang et al. (2014) sampled IN concentration at different altitudes on the Huangshan Mountains in Southeast China using three mixing cloud chambers and a static diffusion cloud chamber. They found that the concentrations of IN decreased with an increase in altitudes and varied with meteorological conditions, with higher IN concentrations often observed on days with strong wind. But, it is still poorly understood how IN concentration is affected by aerosol properties, especially in southern China, where the concentration of air pollutants having been increasing rapidly during the last decades due to the rapid economy development. Therefore, it has an important significance to study atmospheric IN characteristics in the region. In this study, the observation site was selected at the top of Huangshan in Southeast China, the highest point in the region and is relatively less affected by local emission. There were no obvious anthropogenic pollution sources for aerosols at the surrounding regions of the observational site.

2. Methodology and instrumentation

The experimental site was located at the Guangmingding peak on Huangshan (118.09°E, 30.08°N, 1840 m a.s.l.). The experiments were conducted from September to October in 2012. In order to measure the number concentration of IN, aerosol particles were collected on a silicon substrate by a newly built high-voltage electrostatic aerosol collector (HVEAC), and were analyzed in a newly built static vacuum vapor diffusion cloud chamber. During the experiments, 10 L of air was pumped with a rate of 2 L min^{-1} through the HVEAC which collects aerosol particles on the silicon substrate of 45 mm in diameter. The sampling was conducted twice daily at 08:00 and 14:00 LST. At the same time, the basic meteorological parameters such as air pressure, temperature, relative humidity, and wind, were measured using an automatic weather station. The concentration of aerosol particles was measured by a TSI Model 3321 Aerodynamic Particle Size (APS) and a Model 3081 Scanning Mobility Particle Size Spectrometer (SMPS). APS measures particles of 0.5–20 μm in diameter, and SMPS measures aerosol particles with size in the range of 0.01–1.0 μm.

The newly built static vacuum vapor diffusion cloud chamber was designed based on the principles of the static vacuum vapor diffusion chamber FRIDGE (Frankfurt Ice Nuclei Deposition Freezing Experiment) (Bundke et al., 2008; Klein et al., 2010) and was built at Nanjing University of Information Science & Technology (Su et al., 2014). This chamber was built for activation, growth, and counting of IN collected on silicon substrates. The main body of the chamber can be separated into upper and lower halves or can be sealed together. The upper part of the chamber is connected to an external water vapor chamber and a suction pump. The water vapor chamber consists of a stainless steel cylinder containing water with a depth of 0.5 cm. Before the experiments, the water vapor chamber was cooled to form ice surface. The bottom of the cloud chamber and the water vapor chamber is equipped with a Palter cooled element and is kept thermostatic by a PID controller. A micro-PT1000 senor is placed near the edge of the substrate to measure the temperature close to the surface of the substrate. On the top of the cloud chamber, a CCD camera is mounted to observe the growth of ice crystals on the substrate illuminated by an LED-ring.

Table 1
The concentrations of IN and the ratios of IN concentration to aerosol particles between 0.5 and 20 μm at different temperatures.

Temperature (°C)	Average concentration of IN (L^{-1})	Maximum concentration of IN (L^{-1})	Minimum concentration of IN (L^{-1})	IN/aerosols (0.5–20 μm) (mean ± std. error of mean)
−15	0.27	0.89	0.11	$(1.7 \pm 2.0) \times 10^{-5}$
−17	0.90	2.22	0.22	$(6.6 \pm 10.3) \times 10^{-5}$
−20	2.03	4.33	0.89	$(1.5 \pm 2.0) \times 10^{-4}$
−23	7.02	11.89	3.78	$(5.5 \pm 7.6) \times 10^{-4}$

Before the experiments, the substrates sampled with aerosols were placed on the bottom of the cloud chamber. Then, the chamber was closed, evacuated by a vacuum suction pump, and cooled to desired temperatures. When the temperature over the substrate surface reached to the required value, the connection of the cloud chamber and the water vapor chamber was switched on to introduce water vapor. IN in the aerosol particles sampled on the substrate began to activate and grow to ice crystals. After activation, pictures of the ice crystals were taken by a CCD camera and the number of ice crystals was counted by software automatically. The supersaturation over the substrate surface was calculated from the temperature of the substrate surface and the ice surface in water vapor chamber. Through precise control of temperature and pressure, the activation and growth of IN can be simulated in this cloud chamber.

3. Results and discussions

3.1. Characteristics of IN concentration and distribution

Table 1 gives the average, maximum, and minimum number concentrations of IN under four temperatures (−15 °C, −17 °C, −20 °C, −23 °C) at 8% of supersaturation with respect to ice (S_i) in the period from September 27 to October 12. The average IN concentration was in the range of 0.27–7.02 L^{-1}, obtained by reducing the temperature from −15 °C to −23 °C. Fig. 1 shows the variations of IN concentration with time during the experimental period at the four different temperatures. It can be seen that, on October 10, the highest values of IN concentration were found at all temperatures. Previous studies indicated that larger aerosols are more conducive to act as IN, especially the particles greater than 0.5 μm in diameter (e.g., Stith et al., 2009; DeMott et al., 2010; Chou et al., 2011). Fig. 2 shows the concentration of aerosol particles measured with the APS and SMPS. It can be seen that the concentration of coarse mode particles (0.5–20 μm) also reached a maximum value on the same day when the concentration of IN was highest. High IN concentration was also observed on October 6 when the aerosol concentration was high. For the small aerosol particles (0.01–0.5 μm) measured with the SMPS, however, there was no peak values of IN corresponding to the maximum aerosol number concentration measured on September 29. The correlation of IN with aerosols in different size ranges can be seen in Table 2. High correlation exists between IN and aerosol particles in the size range of 0.5–20 μm for all temperatures, and square correlation coefficients (R^2) between IN and coarse aerosol particles (0.5–20 μm in diameter) were all higher than 0.60, much higher than that (0.10) between IN and smaller particles (0.01–0.5 μm). Therefore, it can be concluded that the large aerosol particles contribute more to IN. Moreover, Table 1 also shows the ratio of IN to the concentration of aerosol particles of 0.5–20 μm in diameter. The magnitude is about 10^{-4}–10^{-5}, indicating that only a very small fraction of atmospheric aerosol particles can act as IN.

During the experiments, the sampling of IN was conducted at 08:00 and 14:00 LST every day. Fig. 3 gives the average concentrations of IN at 08:00 and 14:00 during the experimental period. Table 3 gives the results of paired samples *T*-test of

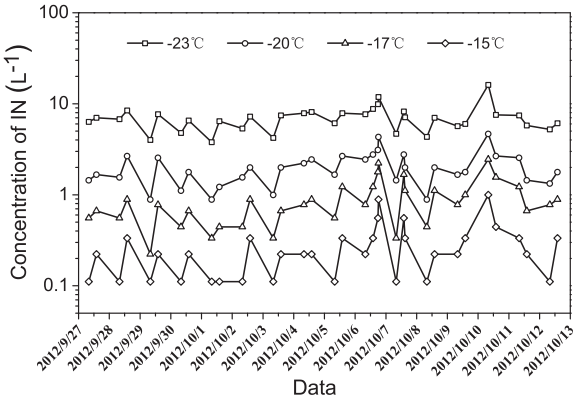

Fig. 1. The changes in the concentrations of IN at different temperatures.

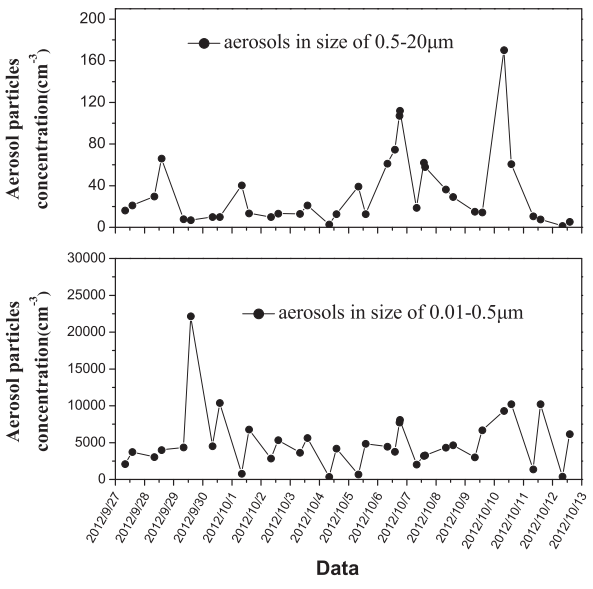

Fig. 2. The variations of the concentration of aerosol particles during the experimental period.

Table 2
The correlation between IN and aerosol particles in different size ranges.

R^2 between IN and aerosols	−15 °C	−17 °C	−20 °C	−23 °C
0.5–20 μm	0.67	0.62	0.60	0.64
0.01–0.5 μm	0.10	0.074	0.11	0.11

IN concentration at 08:00 AM and 14:00 PM, and computes some kind of "Student t" tests and calculates the "p" scores to compare the difference of IN concentration at 08:00 AM and 14:00 PM. From Table 3, we can see that the "p" scores are less than the 5% significance level. Therefore, it can be concluded that the concentration of IN at 14:00 PM is significantly higher than that at 08:00 AM. This is consistent with the daily variation of the concentration of aerosol particles and is correlated with the variations of the boundary layer height (Chen et al., 2011).Chen et al. (2011) showed that the solar radiation reached maximum at about 14:00 PM. Since the solar radiation heated the surface under the top of the mountain, strengthening of the turbulent mixing in boundary layer led to the diffusion of atmospheric aerosols by atmospheric turbulence. Aerosol particles were transported from the foot of the mountain to the observation site on the top, resulting in higher aerosol concentration at 14:00 PM. Meanwhile, IN concentration could also be impacted by valley wind. In daytime wind direction was towards the top of the mountain, which led to the increase of aerosol concentration on the sampling site.

As we all know, precipitation has a scavenging effect on atmospheric aerosols. Similarly, precipitation also has a scavenging effect on IN. During the experiment period, there was a precipitation process on September 21 to 22. Fig. 4 shows the rainfall intensity during that precipitation event. The hourly rain amount reached a maximum of 4.8 mm at 3:00 on September 22. The concentrations of IN before and after the precipitation were shown in Fig. 5. The samplings taken at 14:00 PM, September 20, or before precipitation and 14:00 PM, September 22, or after precipitation show that the concentration of IN after precipitation was much lower than before, indicating that the precipitation had a clear scavenging effect on IN (see also in Fig. 6).

3.2. Dependence of IN concentration on temperature, aerosol particles and ice supersaturation

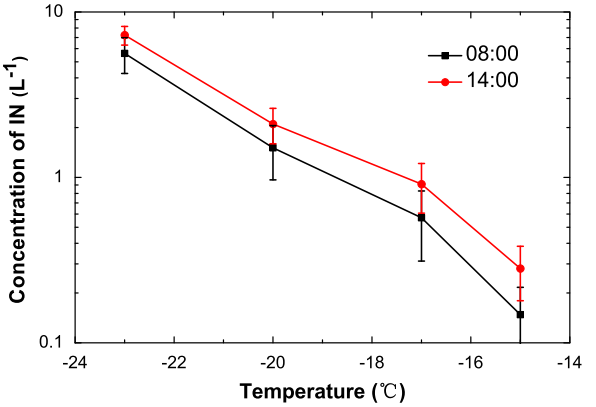

Fig. 3. The average concentrations of IN at 08:00 and 14:00 LST during the experimental period. The error bars represent the standard deviation.

Temperature and the supersaturation with respect to ice (S_i) are the two main parameters which determine ice nucleation. Huffman (1973) showed that S_i is a good parameter to characterize the deposition nucleation in observations of IN. In this study, all the samples were analyzed under conditions supersaturated with respect to ice and subsaturated with respect to liquid water. Therefore, only the deposition IN was quantified. Fig. 7(A) and (B) shows the variations of IN with supersaturation and temperature of a three dimensional plot representing concentration of IN for different supersaturations and temperatures. It is clearly seen that the concentration of deposition IN increases with decreasing temperature and increasing supersaturation.

The dependence of IN concentration to supersaturation has been studied by many researchers (e.g. Al-Naimi and Saunders, 1985; López and Ávila, 2013; Patade et al., 2014). Fig. 8 shows the variation of IN concentration with S_i at different temperatures. In order to compare the present results with previous studies, the data were grouped in three different ranges of temperature: −15 °C to −18 °C, −18 °C to −20 °C, and −20 °C to −23 °C. Fig. 8 compares the results obtained in the present work with the experimental data reported by Al-Naimi and Saunders (1985), López and Ávila (2013) and Patade et al. (2014). The measurement of IN concentration reported by Al-Naimi and Saunders (1985) was carried out with a continuous flow diffusion chamber at different temperatures and supersaturations. López and Ávila (2013) measured natural deposition ice nuclei in Argentina using a cloud chamber cooled by sudden expansion of air. Patade et al. (2014) used a thermal gradient diffusion chamber (TGDC) to activate the IN by deposition mode over ice supersaturation of 6–24% and at a temperature of −18.5 to −13.5 °C. From Fig. 8 we can see that all the experimental results, including the present one, show the exponential dependence of IN on S_i, although these experimental data were conducted from different instruments over different locations. The present results are within the range of previous studies.

The dependence of IN concentration of temperature has been shown by numerous authors (e.g. Fletcher et al., 1962; Hussain and Saunders, 1984; Meyers et al., 1992; DeMott et al., 2010). In order to analyze the behavior of IN concentration with temperature, the data were grouped for three different ranges of supersaturation: 4%–8%, 8%–15%, and 15%–25%. Fig. 9 shows the variation of IN concentration with temperature under different S_i and a comparison of the present work with previous studies by Al-Naimi and Saunders (1985) and López and Ávila (2013). As can be seen in Fig. 9, the IN concentrations in this work are consistent with those previously reported results. All the experimental points behave with the same trend and the IN concentration increases with a decrease in temperature.

Previous studies (e.g., Meyers et al., 1992; DeMott et al., 2003; Pruppacher et al., 1998) found that the IN concentration increases nearly exponentially with decreasing temperature. A convenient approximation of the behavior (Fletcher et al., 1962) is

$$N = N_0 \times \exp(-b \times T) \quad (1)$$

where T is the activation temperature, N is the number concentration of activated IN under temperature T, N_0 and b are the empirical parameters, and N_0 represents the IN

Table 3
The results of paired samples *T*-test of IN concentration at 08:00 AM and 14:00 PM.

		Paired differences					t	df	Sig. (2-tailed)
		Mean	Std. deviation	Std. error of mean	95% confidence interval of the difference				
					Lower	Upper			
−15 °C	08:00–14:00	−.13333	.12738	.032289	−.20387	−.06279	−4.054	14	.001
−17 °C	08:00–14:00	−.34074	.40601	.10483	−.56558	−.11590	−3.250	14	.006
−20 °C	08:00–14:00	−.5259	.66357	.17133	−.96007	−.22512	−3.459	14	.004
−23 °C	08:00–14:00	−1.62963	1.43751	.37116	−2.42570	−.83356	−4.391	14	.001

concentration when the temperature is 0 °C. The parameter *b* varies from about 0.3 to 0.8 $(°C)^{-1}$ (Levin and Cotton, 2009).

In order to analyze quantitatively the relationship between IN concentration and temperature, Fig. 10 shows the concentration of IN obtained in this study as a function of temperature under a certain supersaturation of 8%. It should be emphasized that this analysis is only to illustrate how IN concentration can be expressed with temperature. The resulting best-fit line can be expressed as

$$N(T) = 0.0004 \times \exp(-0.4208 \times T) \quad (2)$$

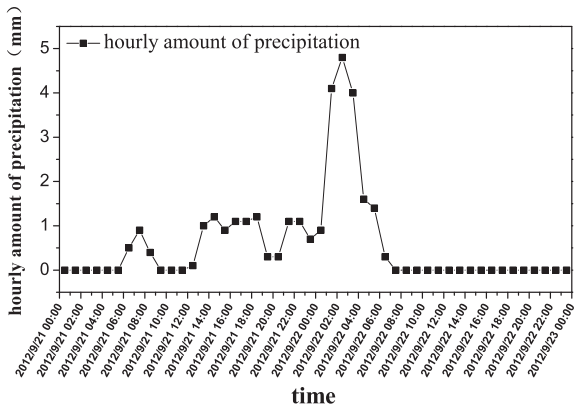

Fig. 4. The changes in rainfall intensity with time on September 21 to 22.

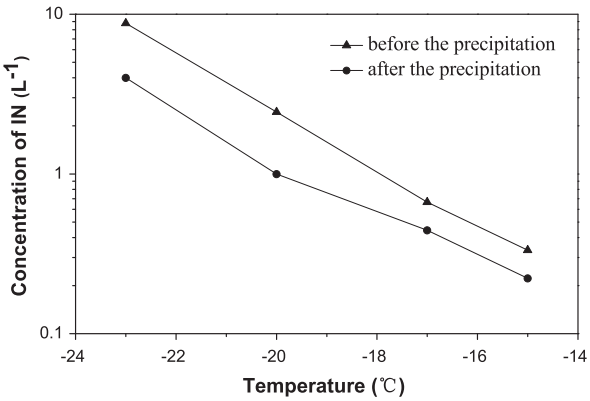

Fig. 5. The concentrations of IN before and after the precipitation process.

where, $N(T)$ is the concentration of IN at temperature T (°C). The units of the two parametric coefficients (0.0004 & −0.4208) are 1/L and $(°C)^{-1}$, respectively. The square of correlation coefficient R^2 is 0.853. The experimental points also exhibited a large variability in IN concentration at a single temperature. This mainly resulted from the difference in aerosol concentration. There are inherent spatial and temporal variations in the concentrations of aerosol particles which can act as IN. For example, the aerosol concentration (0.5–20 μm) is up to about 180 cm^{-3} on some days, while sometimes only about 10 cm^{-3} (see Fig. 2).

DeMott et al. (2010) found that a correlation exists between the observed IN concentrations and the number concentration of aerosol particles larger than 0.5 μm in diameter, and showed a parameterization depending on both the activation temperature and the concentration of aerosol particles. In order to analyze the dependence of IN concentration on aerosol concentration on this mountainous site, we also attempted to establish a parametric relationship (Eq. (3)) relating IN concentration with temperature and the concentration of aerosol particles,

$$N\left(T, n_{aer,0.5\ \mu m}\right) = 5.607 \times 10^{-12}(-T)^{8.721}\left(n_{aer,0.5\ \mu m}\right)^{(0.019T+0.579)} \quad (3)$$

where, T is the activation temperature, $n_{aer,0.5\ \mu m}$ is the concentration (cm^{-3}) of aerosol particles with diameter larger

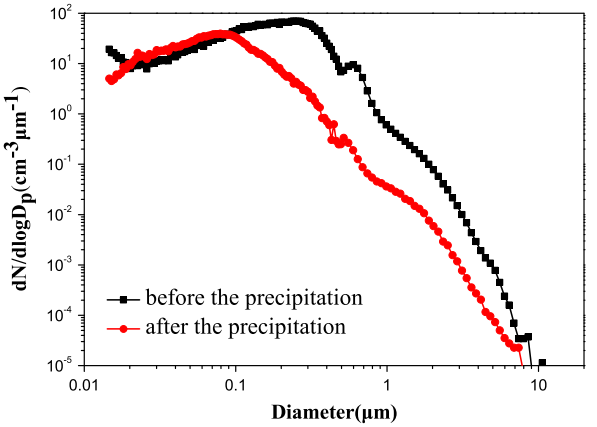

Fig. 6. The spectral distributions of the aerosol particles before and after precipitation.

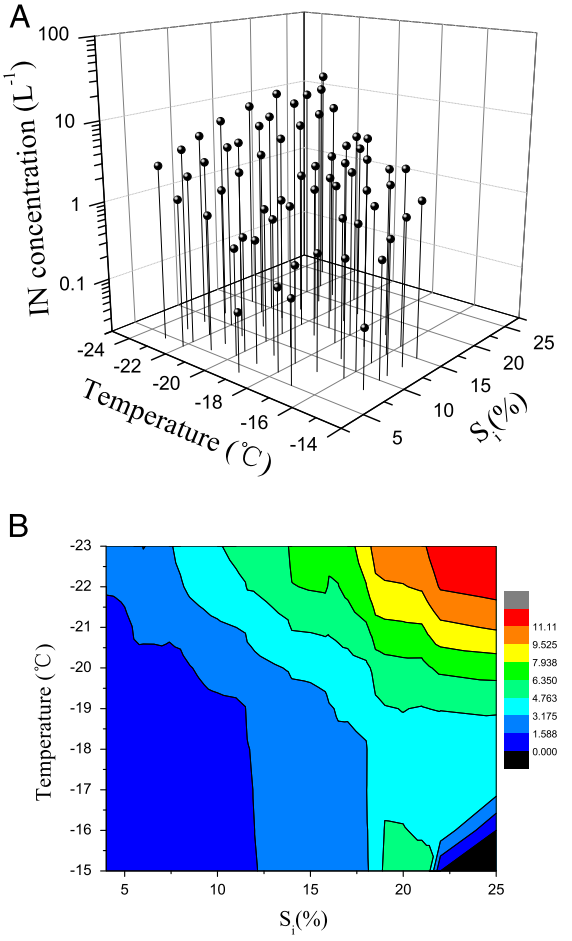

Fig. 7. (A) Three dimensional plot representing concentration of IN changing with supersaturation and temperature, (B) the corresponding interpolated data in color scale.

than 0.5 μm, and $N(T, n_{aer,0.5\ \mu m})$ is the concentration of IN when the activation temperature is T and the concentration of aerosol particles (0.5–20 μm) is $n_{aer,0.5\ \mu m}$. The square of correlation coefficient R^2 is 0.889, slightly higher than that only temperature was considered ($R^2 = 0.853$).

Fig. 11 shows a comparison of the observed and calculated IN concentrations based on Eqs. (2) and (3), respectively. In Fig. 11, the solid line represents the ratio of calculated and observed values of 1:1. In Fig. 11A, the calculated IN concentration when only temperature was considered is based on Eq. (2). This relation is biased more above the 1:1 line. In Fig. 11B, calculations are based on Eq. (3), which depends on both $n_{aer,0.5\ \mu m}$ and T. This parameterization shows less bias along the 1:1 line. The deviation between calculated and observed values based on temperature is larger than that based on both temperature and aerosols. It is more reasonable to consider both temperature and aerosol particles with diameters larger than 0.5 μm.

Although we found the dependence on IN concentration of temperature, supersaturation and aerosol concentration, we think that it is valuable to obtain a parametric equation for deposition ice nuclei concentrations in such a mountain site, something that could be helpful in numerical models. Meyers et al. (1992) suggested that a parameterization of IN as a function of temperature and supersaturation is:

$$N = \exp(-0.639 + 0.1296 \times S_i) \tag{4}$$

which is performed by using the data of Rogers (1982) and Al-Naimi and Saunders (1985).

Based on the parameterizations of Fletcher et al. (1962) and Meyers et al. (1992), the results obtained in this study are parameterized by combining Eqs. (1) and (4) as follows:

$$N = A\exp(B \times T + C \times S_i) \tag{5}$$

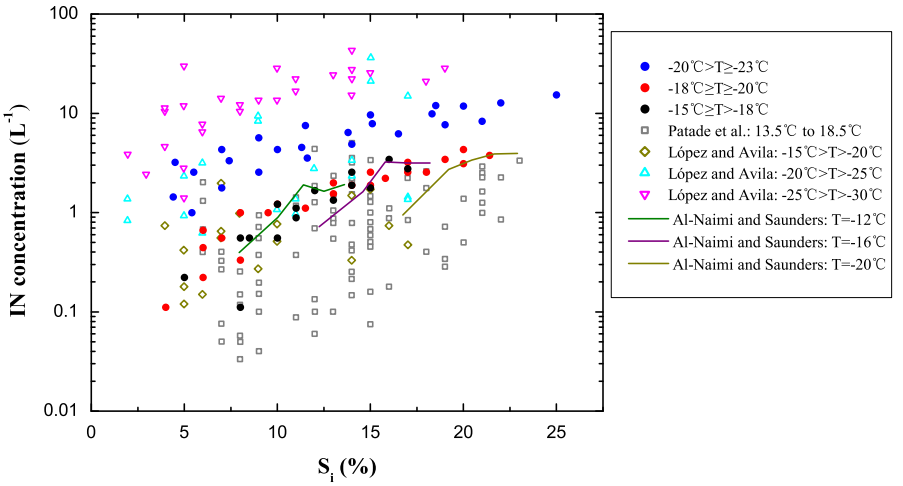

Fig. 8. The variations of IN concentration with S_i at different temperatures. Some of the results obtained in previous studies are also shown for comparison.

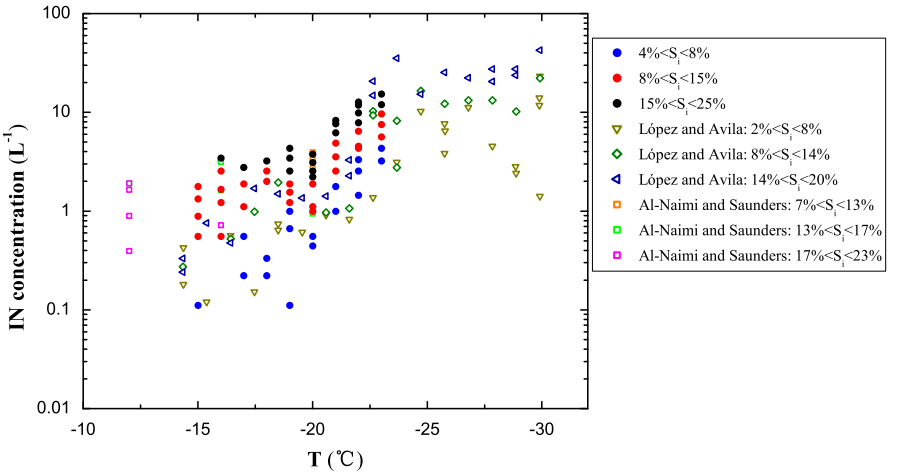

Fig. 9. The variations of IN concentration with temperature at different supersaturations (S_i). Some of the results obtained in previous studies are also shown for comparison.

where A, B and C are the constant parameters, and T and S_i are in °C and %, respectively.

According to Eq. (5), a parameterization by fitting the experimental data is given by

$$N(T, S_i) = 0.0026 \exp(-0.254T + 0.138 \times S_i). \quad (6)$$

The square of the correlation coefficient R^2 is 0.778. This fit is reasonably good and may be used in models.

4. Summary and conclusions

To understand the characteristics of IN in background regions in Southeast China, where measurement of IN is absent, a field experiment was conducted on the top of Huangshan (known as the Yellow Mountains), the highest mountain in Southeast China, to measure the physical and chemical properties of aerosol particles and their abilities to act as cloud

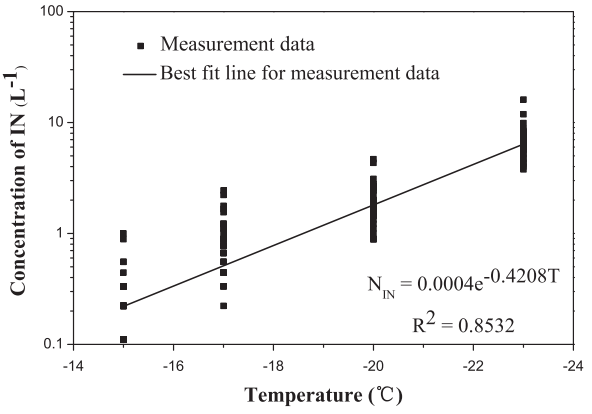

Fig. 10. Average activation spectra of IN (number of IN as a function of temperature). The equation represents the best fit line to the measurement data.

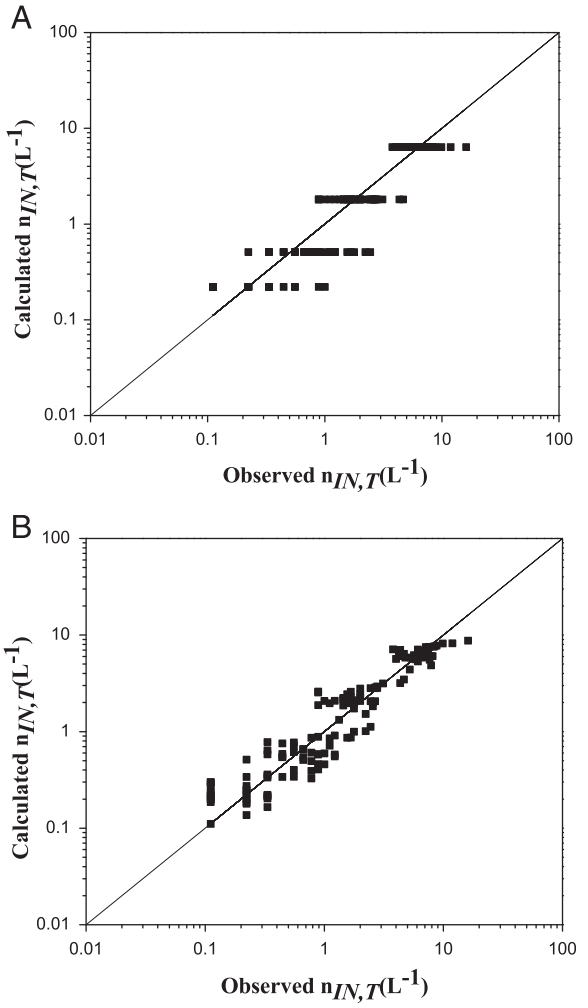

Fig. 11. A comparison of calculated and observed IN concentrations based on two different parameterizations. A is based on Eq. (2), and B is based on Eq. (3).

condensation nuclei (CCN) and atmospheric IN. This paper reports the characteristics of IN measured with a newly built static vacuum water vapor diffusion chamber. The experiments were conducted under temperatures between −15 °C and −23 °C and supersaturation with respect to ice between 4% and 25%. The results show that the average IN concentration was in the range of 0.27 to 7.02 L^{-1}, when the temperature was varied from −15 °C to −23 °C. These results are with the range of previous studies (e.g. DeMott et al., 2003). High correlation of IN with aerosol particle in size of 0.5–20 μm was found for all measured temperatures. The concentration of ice nuclei at 14:00 was significantly higher than that at 08:00. This is consistent with the daily variation of the concentration of aerosol particles at the same location (Chen et al., 2011) and is believed to be associated with the variations of the boundary layer height, and the mountain–valley wind. The boundary layer height changes with solar radiation, which reached maximum around 14:00 PM. The solar radiation heated the slopes of the mountain, strengthening of the turbulent mixing in boundary layer and led to more efficient diffusion of atmospheric aerosols by atmospheric turbulence. Meanwhile, IN concentration could also be impacted by valley wind. In daytime wind direction was towards the top of the mountain, which led to the increase of aerosol concentration on the sampling site.

Anyway, this is the first attempt to characterize IN in a background region in Southeast China. The relationships established in this study, between IN, temperature, supersaturation and the concentration of aerosol particles, may be used in models, but these expressions are also subjected to modification with the increase in data from different time and locations.

Acknowledgments

This study was jointly sponsored by the National Science Foundation of China (Grant No. 41030962), the Special Fund for Doctorate Programs in Chinese Universities (Grant No. 20113228110002), the Priority Academic Program of Development of Jiangsu Higher Education Institutions (PAPD), and the Colleges and Universities in Jiangsu Province plans to graduate research and innovation (Grant No. KYZZ_0243). The authors thank Prof. Heinz Bingemer and Dr. Holger Klein from Institute for Atmospheric and Environmental Sciences, Goethe University, Germany, and Prof. Zev Levin, Tel Aviv University, Israel, for their kind help in building the cloud chamber.

References

Al-Naimi, R., Saunders, C.P.R., 1985. Measurements of natural deposition and condensation–freezing ice nuclei with a continuous flow chamber. Atmos. Environ. 19, 1871–1882.

Archuleta, C.M., DeMott, P.J., Kreidenweis, S.M., 2005. Ice nucleation by surrogates for atmospheric mineral dust and mineral dust/sulfate particles at cirrus temperatures. Atmos. Chem. Phys. 5, 2617–2634.

Ardon-Dryer, K., Levin, Z., Lawson, R.P., 2011. Characteristics of immersion freezing nuclei at the South Pole station in Antarctica. Atmos. Chem. Phys. 11, 4015–4024. http://dx.doi.org/10.5194/acp-11-4015-2011.

Belosi, F., Santachiara, G., Prodi, F., 2014. Ice-formation nuclei in Antarctica: new and past measurements. Atmos. Res. 145–146, 105–111.

Bigg, E.K., 1957. A new technique for counting ice-forming nuclei in aerosols. Tellus 9, 394–400.

Bigg, E.K., 1973. Ice nucleus measurements in remote areas. J. Atmos. Sci. 30, 1153–1157.

Bundke, U., Nillius, B., Jaenicke, R., Wetter, T., Klein, H., Bingemer, H., 2008. The fast ice nucleus chamber FINCH. Atmos. Res. 90, 180–186.

Chen, J., Yin, Y., Lin, Z., Chen, K., Kang, H., Yan, J., 2011. An observational study of aerosol optical properties at the top of Huangshan Mountains. Clim. Environ. Res. 16, 641–648 (in Chinese with English abstract).

Chou, C., Stetzer, O., Weingartner, E., Jurányi, Z., Kanji, A., Lohmann, U., 2011. Ice nuclei properties within a Saharan dust event at the Jungfraujoch in the Swiss Alps. Atmos. Chem. Phys. 11, 4725–4738.

Cozic, J., Mertes, S., Verheggen, B., Cziczo, D.J., Gallavardin, S.J., Walter, S., Baltensperger, U., Weingartner, E., 2008. Black carbon enrichment in atmospheric ice particle residuals observed in lower tropospheric mixed phase clouds. J. Geophys. Res. 113, D15209.

Cziczo, D.J., Froyd, K.D., Hoose, C., Jensen, E.J., Diao, M., Zondlo, M.A., Smith, J.B., Twohy, C.H., Murphy, D.M., 2013. Clarifying the dominant sources and mechanisms of cirrus cloud formation. Science 340, 1320–1324.

DeMott, P.J., Cziczo, D.J., Prenni, A.J., Murphy, D.M., Kreidenweis, S.M., D.M., Thomson, D.S., Borys, R., Rogers, D.C., 2003. Measurements of the concentration and composition of nuclei for cirrus formation. PNAS 100, 14,655–14,660.

DeMott, P.J., Prenni, J., Liu, X., Kreidenweis, S.M., Petters, M.D., Twohy, C.H., Richardson, M.S., 2010. Predicting global atmospheric ice nuclei distributions and their impacts on climate. Proc. Natl. Acad. Sci. U. S. A. 107, 17–22.

Durant, A.J., Shaw, R.A., Rose, W.I., Mi, Y., Ernst, G.G.J., 2008. Ice nucleation and overseeding of ice in volcanic clouds. J. Geophys. Res. 113 D09206.

Field, P.R., Möhler, O., Conolly, P., Krämer, M., Cotton, R., Heymsfield, A.J., Saathoff, H., Schnaiter, M., 2006. Some ice nucleation characteristics of Asian and Saharan desert dust. Atmos. Chem. Phys. 6, 2991–3006. http://dx.doi.org/10.5194/acp-6-2991-2006.

Fletcher, N.H., Souires, P., Bowen, E.G., 1962. The Physics of Rainclouds. Cambridge University Press, (408 pp.).

Froyd, K.D., Murphy, D.M., Lawson, P., Baumgardner, D., Herman, R.L., 2010. Aerosols that form subvisible cirrus at the tropical tropopause. Atmos. Chem. Phys. 10, 209–218.

Gierens, K., 2003. On the transition between heterogeneous and homogeneous freezing. Atmos. Chem. Phys. 3, 437–446.

Haag, W., Kärcher, B., 2004. The impact of aerosols and gravity waves on cirrus clouds at midlatitudes. J. Geophys. Res. 109, D12202. http://dx.doi.org/10.1029/2004JD004579.

Hallett, J., Mason, B.J., 1958. The influence of temperature and supersaturation on the habit of ice crystals grown from the vapour. Proc. R. Soc. A 247, 440–453.

Hoyle, C.R., Pinti, V., Welti, A., Zobrist, B., Marcolli, C., Luo, B., Hoskuldsson, A., Mattsson, H.B., Thorsteinsson, T., Larsen, G., Peter, T., 2011. Ice nucleation properties of volcanic ash from Eyjafjallajokull. Atmos. Chem. Phys. 11, 9911–9926.

Hoose, C., Möler, O., 2012. Heterogeneous ice nucleation on atmospheric aerosols: a review of results from laboratory experiments. Atmos. Chem. Phys. 12, 9817–9854.

Huffman, P.J., 1973. Supersaturation spectra of AgI and natural ice nuclei. J. Appl. Meteorol. 12, 1080–1087.

Hussain, K., Saunders, C.P.R., 1984. Ice nucleus measurement with a continuous flow chamber. Q. J. R. Meteorol. Soc. 110, 75–84.

Jiang, H., Yin, Y., Yang, L., Yang, S.Z., Su, H., Chen, K., 2014. The characteristics of atmospheric ice nuclei measured at different altitudes in the Huangshan Mountains in Southeast China. Adv. Atmos. Sci. 31, 396–406. http://dx.doi.org/10.1007/s00376-013-3048-5.

Junge, K., Swanson, B.D., 2008. High-resolution ice nucleation spectra of sea-ice bacteria: implications for cloud formation and life in frozen environments. Biogeosciences 5, 865–873. http://dx.doi.org/10.5194/bg-5-865-2008.

Kärcher, B., 2004. Cirrus clouds in the tropical tropopause layer: role of heterogeneous ice nuclei. Geophys. Res. Lett. 31, L12101. http://dx.doi.org/10.1029/2004GL019774.

Klein, H., Haunold, W., Bundke, U., Nillius, B., Wetter, T., Schallenberg, S., Bingemer, H., 2010. A new method for sampling of atmospheric ice nuclei with subsequent analysis in a static diffusion chamber. Atmos. Res. 96, 218–224.

Knopf, D.A., Koop, T., 2006. Heterogeneous nucleation of ice on surrogates of mineral dust. J. Geophys. Res. 111, D12201. http://dx.doi.org/10.1029/2005JD006804.

Knopf, D.A., Alpert, P.A., Wang, B., Aller, J.Y., 2011. Stimulation of ice nucleation by marine diatoms. Nat. Geosci. 4, 88–90.

Levin, Z., Cotton, W.R., 2009. Aerosol Pollution Impact on Precipitation: A Scientific Review. Springer.

Lohmann, U., Kärcher, B., Hendricks, J., 2004. Sensitivity studies of cirrus clouds formed by heterogeneous freezing in the ECHAM GCM. J. Geophys. Res. 109, D16204.

Lohmann, U., Stier, P., Hoose, C., Ferrachat, S., Kloster, S., Roeckner, E., Zhang, J., 2007. Cloud microphysics and aerosol indirect effects in the global climate model ECHAM5-HAM. Atmos. Chem. Phys. 7, 3425–3446.

López, M.L., Ávila, E.E., 2013. Measurements of natural deposition ice nuclei in Córdoba, Argentina. Atmos. Chem. Phys. 13, 3111–3119.

Meyers, M.P., DeMott, P.J., Cotton, W.R., 1992. New primary ice-nucleation parameterizations in an explicit cloud model. J. Appl. Meteorol. 31, 708–721.
Murray, B.J., Wilson, T.W., Broadley, S.L., Wills, R.H., 2010. Heterogeneous freezing of water droplets containing kaolinite and montmorillonite particles. Atmos. Chem. Phys. 11, 4191–4207.
Niedermeier, D., Hartmann, S., Shaw, R.A., Covert, D., Mentel, T.F., Schneider, J., Poulain, L., Reitz, P., Spindler, C., Clauss, T., Kiselev, A., Hallbauer, E., Wex, H., Mildenberger, K., Stratmann, F., 2010. Heterogeneous freezing of droplets with immersed mineral dust particles measurements and parameterization. Atmos. Chem. Phys. 10, 3601–3614. http://dx.doi.org/10.5194/acp-10-3601-2010.
Patade, S., Nagare, B., Wagh, S., Maherskumar, R.S., Prabha, T.V., Kumar, P.P., 2014. Deposition ice nuclei observations over the Indian region during CAIPEEX. Atmos. Res. 149, 300–314.
Pratt, K.A., DeMot, P.J., French, J.R., Wang, Z., Westphal, D.L., Heymsfield, A.J., Twohy, C.H., Prenni, A.J., Prather, K.A., 2009. In situ detection of biological particles in cloud ice-crystals. Nat. Geosci. 2, 398–401.
Pratt, K.A., Heymsfield, A.J., Twohy, C.H., Murphy, S.M., DeMott, P.J., Hudson, J.G., Subramanian, R., Wang, Z., Seinfeld, J.H., Prather, K.A., 2010. Situ chemical characterization of aged biomass-burning aerosols impacting cold wave clouds. J. Atmos. Sci. 67, 2451–2468.
Prenni, A.J., Petters, M.D., Kreidenweis, S.M., Heald, C.L., Martin, S.T., Artaxo, P., Garland, R.M., Wollny, A.G., Pöschl, U., 2009. Relative roles of biogenic emissions and Saharan dust as ice nuclei in the Amazon basin. Nat. Geosci. 2, 402–405.
Pruppacher, H.R., Klett, J.D., 1997. Microphysics of Clouds and Precipitation, 2nd ed. Kluwer Academic, pp. 309–360.
Pruppacher, H.R., Klett, J.D., Wang, P.K., 1998. Microphysics of clouds and precipitation. Aerosol Sci. Technol. 28, 381–382.
Roberts, P., Hallett, J., 1968. A laboratory study of the ice nucleating properties of some mineral particulates. Q. J. R. Meteorol. Soc. 94, 25–34.
Rogers, D.C., 1982. Field and Laboratory Studies of Ice Nucleation in Winter Orographic Clouds. (Ph.D. dissertation) Dept. of Atmospheric Science, Univ. of Wyoming, Laramie (161 pp.).
Rogers, D.C., 1988. Development of a continuous flow thermal gradient diffusion chamber for ice nucleation studies. Atmos. Res. 22, 149–181.
Saxena, V.K., Weintraub, D.C., 1988. Ice forming nuclei concentrations at Palmer Station, Antarctica. Atmos. Aerosols Nucleation 309, 679–682.
Steinke, I., Mohler, O., Kiselev, A., Niemand, M., Saathoff, H., Schnaiter, M., Skrotzki, J., Hoose, C., Leisner, T., 2011. Ice nucleation properties of fine ash particles from the Eyjafjallajokull eruption in April 2010. Atoms. Chem. Phys. 11, 12945–12958.
Stith, J.L., Ramanathan, V., Cooper, W.A., DeMott, P.J., Carmichael, G., Hatch, C.D., Adhikary, B., Twohy, C.H., Rogers, D.C., Baumgardner, D., Prenni, A.J., Campos, T., Gao, R., Anderson, J., Feng, Y., 2009. An overview of aircraft observations from the Pacific Dust Experiment campaign. J. Geophys. Res. 114, D05207–D05222.
Su, H., Yin, Y., Lu, C., Jiang, H., Yang, L., 2014. Development of new diffusion cloud chamber type and its observation study of ice nuclei in the Huangshan area. Chin. J. Atmos. Sci. 38, 386–389 (in Chinese with English abstract).
Wang, B., Lambe, A.T., Massoli, P., Onasch, T.B., Davidovits, P., Worsnop, D.R., Knopf, D.A., 2012. The deposition ice nucleation and immersion freezing potential of amorphous secondary organic aerosol: pathways for ice and mixed-phase cloud formation. J. Geophys. Res. 117, D16209.
Wise, M.E., Baustian, K.J., Koop, T., Freedman, M.A., Jensen, E.J., Tolbert, M.A., 2012. Depositional ice nucleation onto hydrated NaCl particles: a new mechanism for ice formation in the troposphere. Atmos. Chem. Phys. 12, 1121–1134.
Zuberi, B., Bertram, A., Cassa, C., Molina, L., Molia, M., 2002. Heterogeneous nucleation of ice in $(NH_4)^2SO_4$–H_2O particles with mineral dust immersion. Geophys. Res. Lett. 29, 1421–1424.